Drosophila Segmentation: Supercomputer Simulation of Prepattern Hierarchy

Axel Hunding
Stuart A. Kauffman
Brian C. Goodwin

SFI WORKING PAPER: 1990--019

SANTA FE INSTITUTE

J. theor. Biol. (1990) **145**, 369-384

Drosophila Segmentation: Supercomputer Simulation of Prepattern Hierarchy

AXEL HUNDING†, STUART A. KAUFFMAN‡‖,
AND BRIAN C. GOODWIN§

† *H. C. Ørsted Institute, University of Copenhagen, Universitetsparken* 5, 2100 *Copenhagen Ø, Denmark,* ‡ *Department of Biophysics, School of Medicine, University of Pennsylvania, Philadelphia, PA* 19104-6059, *U.S.A.,* ‖ *Santa Fe Institute, Santa Fe, New Mexico, U.S.A. and* §*Department of Biology, The Open University, Milton Keynes MK7 6AA, U.K.*

(*Received on* 8 *September* 1989, *Accepted in revised form on* 9 *March* 1990)

Spontaneous prepattern formation in a two level hierarchy of reaction-diffusion systems is simulated in three space co-ordinates and time, mimicking gap gene and primary pair-rule gene expression. The model rests on the idea of Turing systems of the second kind, in which one prepattern generates position dependent rate constants for a subsequent reaction-diffusion system. Maternal genes are assumed responsible for setting up gradients from the anterior and posterior ends, one of which is needed to stabilize a double period prepattern suggested to underly the read out of the gap genes. The resulting double period pattern in turn stabilizes the next prepattern in the hierarchy, which has a short wavelength with many characteristics of the stripes seen in actual primary pair-rule gene expression. Without such hierarchical stabilization, reaction-diffusion mechanisms yield highly patchy short wave length patterns, and thus unreliable stripes. The model yields seven stable stripes located in the middle of the embryo, with the potential for additional expression near the poles, as observed experimentally. The model does not rely on specific chemical reaction kinetics, rather the effect is general to many such kinetic schemes. This makes it robust to parameter changes, and it has good potential for adapting to size and shape changes as well. The study thus suggests that the crucial organizing principle in early *Drosophila* embryogenesis is based on global field mechanisms, not on particular local interactions.

1. Introduction

Early embryonic pattern formation in *Drosophila* (Ingham, 1988) has recently attracted much attention as a possible rosetta stone for pattern formation in animals (Slack, 1984). The discovery (Hafen *et al.*, 1984) of a seven stripe prepattern of the *fushi tarazi* gene prompted several theoreticians to point out the analogy of this phenomenon to Turing structures (Turing, 1952), i.e. prepatterns arising spontaneously by autocatalytic biochemical reaction-diffusion (RD) systems (Goodwin & Kauffman, 1989; Hunding, 1986, 1989; Lacalli *et al.*, 1988; Nagorcka, 1988).

Early models of *Drosophila* embryogenesis based on Turing prepatterns were shown by computer simulation to yield unreliable patchy patterns (Kauffman *et al.*, 1978; Bunow *et al.*, 1980). Stable stripe formation may result, however, if a rate constant in the RD system varies along an imposed gradient (Meinhardt, 1982;

0022-5193/90/017369+16 $03.00/0

in the *oscar* group of genes is set up from the posterior pole. The nature of the mechanism for the emergence of these gradients is not part of the present model. Recent experiments suggest that they arise from maternal genes, with repression of *bicoid* by the gene *nanos* from the posterior pole. In the hierarchical model, only one of these gradients is needed as stabilizer for the next level (the gap gene prepattern).

It is thus assumed that initially one or more gradients exist along the anterior posterior axis, which alter rate constants in a RD system which in turn provides the basis for gap gene expression. The maternal gradient is necessary in this RD system to stablize a prepattern with a wave length half the length of the embryo which we will call a doubly periodic prepattern.

In [Fig. 1(a)] 3-D computer simulation of the emergence of this doubly periodic prepattern (the gap gene prepattern) is shown. If no maternal gradients are present, a patchy pattern obtains, [Fig. 1(c)]. With maternal gradient(s), stablization of a reliable, doubly periodic prepattern occurs, [Fig. 1(a)]. Shown here is one of the components in the RD system, which has high concentration in the middle of the embryo, and close to the poles, with minima in between. This prepattern is assumed to trigger initial expression of the gene *Krüppel*, as this is experimentally known to occur with its main expression in a band in the middle of the embryo, and some

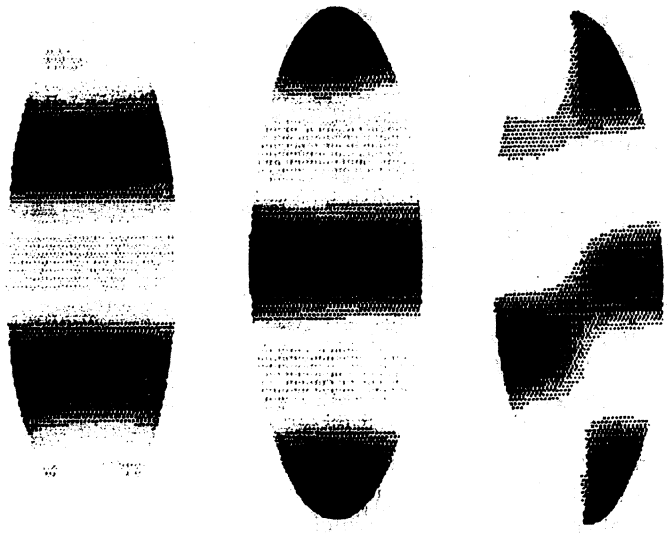

FIG. 1. Gap gene prepattern, generated by simulation of reaction-diffusion (RD) system in three dimensions (elliptical cylinder co-ordinates). A stable bipolar $\cos(4\theta)$ pattern emerges. In this two component Turing system (Selkovs model, see Appendix) one morphogen concentration is high, where the other is low. The prepatterns resemble *Krüppel* expression (a) with a band in the middle and possibilities for expression near the poles, and *hunchback* (or *knirps*), (b) with two bands anterior and posterior to the *Krüppel* centre band. This double period pattern needs maternal gradients (*bic* or *osc*) to be stabilized. In combined *bic-/osc-* mutants, an unpredictable patchy pattern emerges instead (c).

expression as well close to the anterior and posterior poles (Harding & Levine, 1988). In [Fig. 1(b)], the other component of the same RD system is shown. This has high concentrations where the former component was low, and so now two bands adjacent to the central *Krüppel* band emerge from this RD component. It is suggested that these bands activate the genes *hunchback* and *knirps*. Initially, *hunchback* appears only at the anterior band, but later (in nuclear cycle 14), this gene is also read out in the posterior band. The gene *knirps* is activated in the posterior band, and to some extent in the anterior band as well initially, with a later (cycle 14), more pronounced anterior expression. It is an asset of the present model that it easily accounts for both anterior and posterior appearance of these two gap genes, and for the expression of *Krüppel* at anterior and posterior poles. No model based on simple gradients from the poles have so far accounted for these experimental observations (Meinhardt, 1986, 1988).

When the gap genes are activated, they soon start to repress each other. Thus *hunchback* inhibits *Krüppel*, and so does *knirps*. Also, *hunchback* and *knirps* repress one another. These interactions may account for the actual final expression of the gap genes, but such interactions are not directly a part of the prepattern model. They tend to stabilize firmly the geometry of the above gap gene prepattern: the bands created by the gap gene read outs may impose variations in the rate constants in the next RD system (see below) in the same fashion as the gap gene prepattern itself.

With the gap gene prepattern established, and the gap gene expression pattern emerging, a new RD system is triggered with rate constants varying spatially with the gap gene pattern. Thus before the final positioning of the gap gene expression, the pair-rule system is activated: the wave length of this RD system is short, and thus prone to yield patchy patterns, if no stabilization is present (see Fig. 5). With the gap gene pattern influencing the rate constants of this short wave length system, however, seven stable stripes form in the middle of the embryo, thus resembling the initial expression of the gene *hairy*, [Fig. 2(a)-(c)]. Note that this prepattern also has high concentration in some regions near the poles, which may account for the experimentally observed expression of *hairy* close to the anterior pole.

This stable stripe prepattern is the central part of the present model, as it accounts for initial primary pair-rule gene read out (the *hairy/runt/eve* system). The model does not require any precise localization of the gap genes at the time of *hairy/runt/eve* activation, they just have to provide a crude doubly periodic stabilization prepattern. This is considered an important argument in favour of the present model, as some others rely on fairly precise localization of the gap gene expressions before they are able to be effective in controlling *hairy/runt/eve* stripe formation. The reader should also note that the transients computed for the present model resemble what is recorded experimentally, i.e. the primary pair-rule genes are first expressed in the centre of the seven stripe region, then stripe formation is recorded adjacent to the central peak, and finally all seven stripes emerge [compare (Fig. 2(b)-(c)].

An important further argument in favour of the present model is that later, when the maternal gradients are gradually diminished, simulating their experimentally

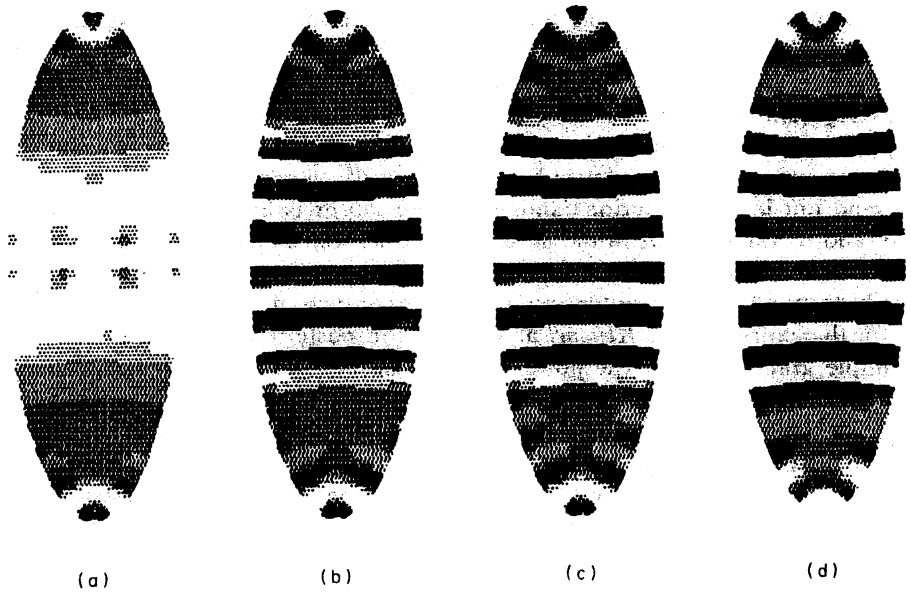

FIG. 2. Primary pair-rule gene stripe prepattern develops in reaction-diffusion system simulations, where the gap gene $\cos(4\theta)$ prepattern (Fig. 1), alters a rate constant in a second RD system, thus stabilizing stripes rather than a patchy pattern. Transients (a)-(b) develop into seven stable stripes (c) in the middle of the embryo. Note additional expression near the poles. Further stripes adjacent to the first seven may emerge, when maternal gradients are removed (d). This prepattern is closely related to actual *hairy/runt* gene expression. The scenario is robust to parameter change of the RD system. It is also common to a broad class of Turing systems, relying on a dynamic geometrical coupling (Turing system of the second kind), rather than specific peculiarities of the reaction-diffusion system kinetics.

recorded disappearance, further stripe formation adjacent to the original seven stripes takes place in the computer simulations, [Fig. 2(d)]. Such additional stripe formation of the *hairy* system is experimentally observed, (see review by Ingham, 1988) and not accounted for by other models so far.

Finally, extensive computer simulations have demonstrated that the formation of seven stripes within the activated centre region is remarkably robust to parameter changes, such as changing rate constants or effective diffusion constants. Also, as stressed already, the mechanism is not dependent on a specific set of chemical reaction mechanisms, but the stabilization of the seven stripes is due to a spatially varying control from the gap gene pattern to the primary pair-rule gene prepattern. Thus this interaction is much more robust to detailed mutational change during evolution, than a mechanism relying on specific biochemical interactions to activate pair-rule genes. Also, a system relying on two interacting RD systems is more reliable with respect to mutations than mechanisms based on only one RD system, which undergoes parameter changes to yield a 1-2-4-8-16- set of periods in the embryo. The reason for this is that in the present two level hierarchical model, mutations in one of the systems will not directly influence the other system, acting only indirectly through spatially varying interaction, which is quite stable. This is especially impor-

tant for the *hairy/runt/eve* system, as its short wavelength makes it comparatively the most vulnerable system to mutations. A direct linkage such as one or more common rate constants in the two RD prepatterns, could have profound effects on the short wavelength RD system. We have made simulations on a single 1-2-4-8-16-model (Fig. 5). These show that such a system is much more prone to yield patchy short wavelength patterns in 3-D calculations, and thus a single RD system seems not reliable as a global field generator for both the gap gene stage and the following short wave length stripes.

3. Simulations of Mutant Patterns

To account for all experimentally observed features of the complex spatial biocybernetic control system operating in *Drosophila* is too much to require at the present stage, as several of the interactions among the relevant genes and their products are still unknown, or only partly known. Simulations of the results of a mutant in which a particular gene is deleted are thus made difficult for several reasons: The missing gene may be important in many other respects, but its deletion may not have much effect on, say, the formation of the gap gene prepattern, as other genes still present may be sufficient for stabilization of this prepattern. Also, effects expected from preliminary models such as the present one may be obscured in the actual embryo by interactions among the genes, which are not so far incorporated in the prepattern theory presented here which mainly focuses on crucial global fields.

With this reservation, the model may be probed with respect to deletion of particular maternal or gap genes. In embryos lacking maternal genes, the maternal gradient system may be changed. Such changes are of crucial importance in the gradient models based on local interactions (Meinhardt, 1986, 1988). We shall give alternative interpretations based on the hierarchical field model. Computer experiments show that only one of the maternal gradients is needed to stabilize the doubly periodic gap gene prepattern. Thus, in *bic-* mutants, or *osc-* mutants, the gap gene prepattern could still form. However, *bicoid* protein is known to activate *hunchback* at three sites of the gene, and thus in *bic-* mutants, *hunchback* is not expressed in its usual anterior band. As *Krüppel* is repressed by *hunchback*, its absence may cause *Krüppel* protein to spread anteriorly as observed.

Similar reasoning may hold for *knirps*, which is repressed by *hunchback*, but *hunchback* is normally repressed in the posterior band by the gene *nanos*. So indirectly, *nanos* activates *knirps* in the posterior band of the gap gene prepattern. As *knirps* also represses *Krüppel*, in *knirps-* mutants the *Krüppel* protein may spread posteriorly, as observed. In combined *bic,-*, *osc-* mutants, both *hunchback* and *knirps* are absent, and *Krüppel* is observed to spread in both directions. In the present model, the absence of both maternal gradients will cause the gap gene prepattern to be patchy, and thus *Krüppel* is not initially confined to its centre band, but may be expressed over large parts of the embryo. A patchy gap gene prepattern, and the lack of subsequent interactions among the gap genes to stabilize a crude double periodic rate constant geometry in the embryo, has profound effects on the next level in the prepattern hierarchy: No stabilization of stripes is possible for the short

wave length pair-rule prepattern, and thus a highly patchy prepattern results in the computer simulations. Consequently, no stripes are formed, and this is what is actually found experimentally in combined *bic-,osc-* mutants (Gaul & Jäckle, 1987; Tautz, 1988; Driever & Nüsslein-Volhard, 1989; Hülskamp *et al.*, 1989).

Gap gene mutants have been extensively studied experimentally, and the resulting embryo is usually smaller for these mutants than the wild type. When the primary pair-rule stripes emerge, however, the mutant embryos are largely of the same size and shape as the wild type. The mutant embryos develop fewer stripes (Ingham *et al.*, 1986), and this is easily explained in the present model by assuming that the gap genes trigger the *hairy/runt/eve* system prepattern by activation of rate constants in this RD system. When a gap gene is missing, the rate constants in the primary pair-rule prepattern are changed, and such changes may easily yield longer wave lengths of the resulting prepattern. Thus, fewer but broader stripes are formed. A computer simulation is shown in [Fig. 3(a)]. This easily accounts for the formation of stripes extending over a larger number of nuclei than in the wild type. This provides support for a global field prepattern mechanism rather than a mechanism based on interactions among a particular number of nuclei by a local mechanism.

FIG. 3. Gap gene mutants are simulated. If such mutants alter rate constants in the primary pair-rule prepattern RD system, (Fig. 2), fewer but broader stripes may evolve (a). Such simulations often yield stripes, which combine to yield a hole in the middle between two fused stripes [indicated by arrow in (b)], and this is indeed observed experimentally. Also, the broadening of stripes is easily achieved in this model, whereas models relying on a specific number of nuclei to interact in a local mechanism have difficulties with encompassing the experimentally observed broadening of the stripes. Thus the hierarchical global field model presented here is able to account for several experimental observations, hitherto not accounted for by other models of local interactions. Parameters used for (a) were $D_1 = 0{\cdot}006$, $\varepsilon_1 = 0{\cdot}36$. For (b) we used $\varepsilon_1 = 0{\cdot}26$.

A further feature of interest is that if the influence from the doubly periodic gap gene prepattern on the RD system of the pair-rule system is reduced, the resulting fewer stripes have a tendency to melt together, forming a hole in the middle. A computer simulation is shown in [Fig. 3(b)]. Such holes are often seen in mutant embryos of the gap genes, and are so far not accounted for by other models. It should be stressed that three-dimensional simulations are important to demonstrate this effect.

A further indication, that a link between the gap genes and the pair-rule system exists, which has so far been unexplored, is stressed by the recent finding (Carroll & Vavra, 1989), that some stripe formation in the pair-rule system seems to be present even in embryos missing all three gap genes (triple gap gene mutants, *Kr-,hb-,kni-*). In the present hierarchical model, this link is the primary pair-rule prepattern, which is assumed to govern actual gene expression.

Further analysis of the effect of missing gap genes would require simulation of interactions of the gap genes and their products (not only the gap gene prepattern) on the various genes in the pair-rule system. Such interactions have not been incorporated in the computer model yet.

The reader may consult recent work about the detailed mechanism for activation of particular stripes, to the extent, that this is so far known (Vavra & Carroll, 1989). We wish to emphasize that non-global models are unlikely to produce reliable stripes. For example, mutual *hairy* and *runt* inhibition may generate a bistable system which could amplify already existing inhomogeneities. However, bistable or even multistable mechanisms would amplify *any* pre-existing inhomogeneity, and thus they bypass the essential point, which is why stripes are created, rather than an ill defined patchy pattern (Akam, 1989). A robust periodic prepattern is needed to make such amplification reliable, and the creation of such a prepattern is precisely what we propose and simulate in this work.

4. Discussion

A major difference between the present model and mechanisms of local interaction is, that the gap genes are not assumed to set up actual boundaries to diffusing substances in the primary pair-rule RD system. Thus the formation of stripes in our model is not linked to any precise linkage of borders between gap gene expression and the pair-rule system. If assumptions are made, that, say, *hairy* is activated on the border of *Krüppel* and *hunchback*, and simulations are carried out for an isolated subregion defined by a gap gene (a cardinal region), this is a silent introduction of compartments in the pair-rule RD system (Meinhardt, 1988). Such compartments are not communicating with each other, as any communication would mean a global model with a short wave length RD system, highly prone to patchy pattern formation. Only by introducing silent compartments is it possible in this way to avoid the break up of the stripes. On the contrary, we believe that the experimental evidence is in support of a very dynamic, *global* stripe formation mechanism, and so stabilization of the RD system over the entire embryo is necessary.

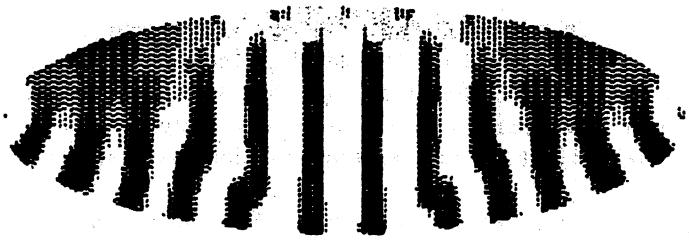

FIG. 4. Dorsal–ventral bending of stripes is possible if a DV gradient is built into effective diffusion coefficients of the *hairy* RD system. Usually the *hairy* stripes bend near the poles of the embryo according to co-ordinates in an elliptical region. The further DV bending is absent in certain *dorsal-* mutants, which may simply mean that the DV gradient is not affecting the *hairy* RD system in these mutants.

The experimental finding that the pair-rule gene stripes bend in regions close to the poles of the embryo, resembling the coordinate system of a three-dimensional ellipsoid, supports a global field model. The further experimental observation that the stripes are restricted to a narrower zone dorsally, and spread out ventrally, may be simulated on the computer by introducing effective diffusion constants (Hunding

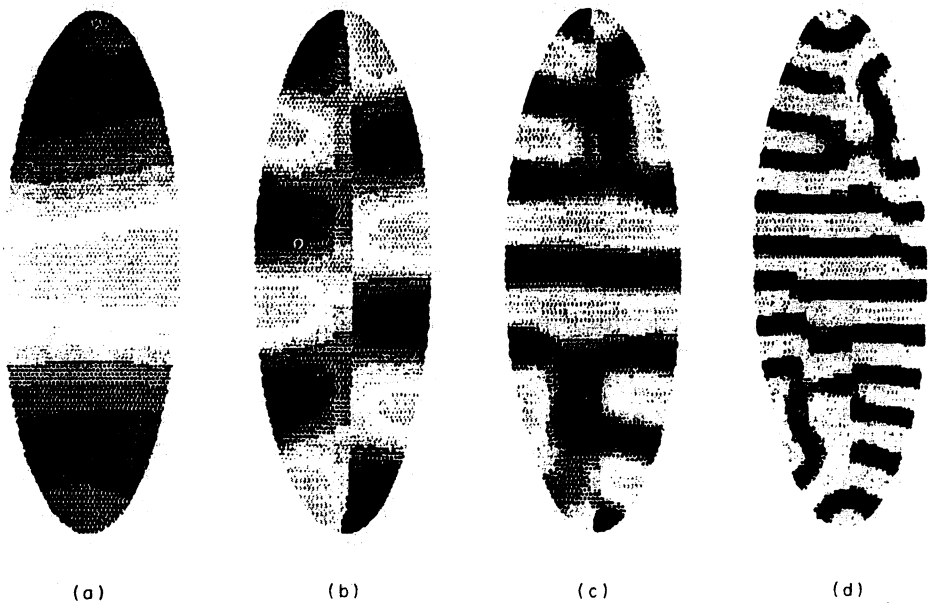

FIG. 5. Unreliable patchy patterns arise in non-hierarchical models, if a single RD system is used and a rate constant is changed to reduce the wavelengths of the emerging patterns. Although an initial stable pattern emerges with a single central peak, i.e. a period 1 pattern (a), successive doubling of the wavelength in a search for period 1-2-4-8- stripes yields highly patchy patterns instead (b)–(d), when simulated in three spatial co-ordinates.

& Sørensen, 1988) which vary along a dorsal-ventral gradient. Such a simulation is seen in (Fig. 4). This fits nicely the experimental observation that this DV variation may be absent in mutants that are defective in one of the genes of the DV system (Carroll *et al.*, 1987).

It has been found experimentally that region specific alleles of the gene *hairy* exist. In these mutants, some of the usual *hairy* stripes are absent (Howard *et al.*, 1988). This has been taken as an argument against a global field mechanism. However, in the present model, where prepatterns (and gene products) from a higher level in the hierarchy control the regions in which stripes form in the RD system lower in the hierarchy, the absence of stripes in certain regions cannot be used to infer that a global mechanism is impossible. A simple explanation could be that the mutants make changes in the rate constants in the higher level hierarchy RD system as well, thus causing the stripes to vanish.

We have summarized the merits of the present global hierarchical field model and a comparison with other model explanations, based on maternal gradients and local interactions in Table 1. Although the present model does not account for all experimental data, examination of the table shows that the present model certainly has its merits, and may be more powerful as a first approximation to the spatial governing principle in *Drosophila* than local models. Any final model, however, is likely to incorporate features of existing local and global models.

TABLE 1

Topic	Hierarchical model	Local model
Both anterior and posterior expression of gap genes *hunchback* and *knirps*	Predicted	Not in other models
Anterior and posterior expression of *Krüppel*	Predicted	Not in other models
Main gap gene expression controlled by maternal genes. Position shift in mutants.	Predicted by prepattern and interacting gap genes	Predicted by maternal gradients and interacting gap genes
Relation between gap and pair-rule patterns	Crude imprecise interactions sufficient	Precise alignment required and incorporated
Stable short wavelength pair-rule stripes rather than patchy pattern	Stable stripes with global control, no compartments	Compartments introduced to stabilise short wave pattern
Isolated nuclei trapped interiorly may express band pattern	Predicted	Impossible in models of interactions among neighbouring nuclei
Gap gene mutants show fewer broadened stripes	Easily accounted for	Not easy with interactions among fixed number of nuclei
Gap gene mutants show melted stripes	Predicted	Not discussed so far
Dorsal-ventral bending of stripes	Possible with DV dependent diffusion constants	Not discussed so far
Missing stripes in *hairy* alleles	Possible with changes above in hierarchy	Not discussed so far
Some pair-rule stripes in mutants lacking all three gap genes (*kr-*, *hb-*, *kni-*)	Possible	Not easy with models dependent on gap gene interactions

REFERENCES

AKAM, M. (1987). *Development* **101**, 1-22.
AKAM, M. (1989). *Nature, Lond.* **341**, 282-283.
BUNOW, B., KERNEVEZ, J.-P., JOLY, G. & THOMAS, D. J. (1980). *J. theor. Biol.* **84**, 629-649.
CARROLL, S. B., WINSLOW, G. M., TWOMBLY, V. J. & SCOTT, M. P. (1987). *Development* **99**, 327-332.
CARROLL, S. B. & VAVRA, S. H. (1989). *Development* **107**, 673-683.
DRIEVER, W. & NÜSSLEIN-VOLHARD, C. (1988). *Cell* **54**, 83-93.
DRIEVER, W. & NÜSSLEIN-VOLHARD, C. (1989). *Nature, Lond.* **337**, 138-142.
GAUL, U. & JÄCKLE, H. (1987). *Cell* **51**, 549-555.
GOODWIN, B. & KAUFFMAN, S. A. (1989). In: *Cell to Cell Signalling: From Experiments to Theoretical Models* (Goldbeter, A., ed.) pp. 213-225. New York: Academic Press.
HAFEN, E., KUROIWA, A. & GEHRING, W. J. (1984). *Cell* **37**, 833-841.
HARDING, K. & LEVINE, M. (1988). *EMBO J.* **5**, 205-214.
HOWARD, K. R. (1989). *Nature, Lond.* **338**, 618-619.
HOWARD, K. R., INGHAM, P. W. & RUSHLOW, C. (1988). *Genes Dev.* **2**, 1037-1046.
HUNDING, A. (1982). In: *Evolution of Order and Chaos in Physics, Chemistry and Biology* (Haken, H., ed.) pp. 100-111. Berlin: Springer Verlag.
HUNDING, A. (1983). *J. math. Biol.* **17**, 223-239.
HUNDING, A. (1989). In: *Cell to Cell Signalling: From Experiments to Theoretical Models* (Goldbeter, A., ed.) pp. 229-235. New York: Academic Press.
HUNDING, A. (1986). In: *Selforganization by Nonlinear Irreversible Processes* (Ebeling, W. & Ulbricht, H., eds) pp. 158-163. Berlin: Springer Verlag.
HUNDING, A. (1987). *J. math. Biol.* **25**, 109-121.
HUNDING, A. & SØRENSEN, P. G. (1988). *J. math. Biol.* **26**, 27-39.
HÜLSKAMP, C., SCHRÖDER, C., PFEIFLE, C., JÄCKLE, H. & TAUTZ, D. (1989). *Nature, Lond.* **338**, 629-636.
INGHAM, P. W. (1988). *Nature, Lond.* **335**, 25-34.
INGHAM, P. W. & GERGEN, P. (1988). *Development* **104** (Suppl.), 51-60.
INGHAM, P. W., HOWARD, K. R. & ISH-HOROWITZ, D. (1985). *Nature, Lond.* **318**, 439-445.
INGHAM, P. W., ISH-HOROWITZ, D. & HOWARD, K. R. (1986). *EMBO J.* **5**, 1659-1665.
JÄCKLE, H., TAUTZ, D., SCHUH, R., SEIFERT, E. & LEHMANN, R. (1986). *Nature, Lond.* **324**, 668-670.
KAUFFMAN, S. A., SHYMKO, R. M & TRABERT, K. (1978). *Science* **199**, 259-270.
LACALLI, T. C., WILKINSON D. A. & HARRISON, L. G. (1988). *Development* **104**, 105-113.
MEINHARDT, H. (1982). *Models of Biological Pattern Formation.* London: Academic Press.
MEINHARDT, H. (1986). *J. Cell Sci.* **4** (Suppl.), 357-381.
MEINHARDT, H. (1988). *Development* **104** (Suppl.), 95-110.
NAGORCKA, B. N. (1988). *J. theor. Biol.* **132**, 277-306.
SEL'KOV, E. E. (1968). *Eur. J. Biochem.* **4**, 79-86.
SLACK, J. (1984). *Nature, Lond.* **310**, 364-365.
TAUTZ, D. (1988). *Nature, Lond.* **332**, 281-284.
TURING, A. M. (1952). *Trans. R. Soc. Lond. Ser B.* **237**, 37-72.
VAVRA, S. H. & CARROLL S. B. (1989). *Development* **107**, 663-672.

APPENDIX

Here, we shall give a brief outline of the equations which are actually solved in the hierarchical field model, and some comments regarding the numerical method used.

Usually, reaction-diffusion systems are of the form;

$$\partial \mathbf{c}/\partial t = \mathbf{F}(\mathbf{c}) + \mathbf{D}\Delta\mathbf{c}. \tag{1}$$

Here, $\mathbf{c}$ is the concentration vector, and the last term is Fickian diffusion. $\mathbf{F}(\mathbf{c})$ contains the chemical kinetic terms, and as already discussed in the above text, the patterns which emerge are largely independent of which model is used for this term.

We have used Sel'kov's scheme (Sel'kov, 1967):

$$F_1 = 1 - c_1 c_2^{\gamma} \tag{2}$$

$$F_2 = \alpha c_1 c_2^{\gamma} - \alpha c_2. \tag{3}$$

The two morphogens have concentrations c_1 and c_2, respectively. α is an enzyme activity (rate constant), and γ is a Hill constant arising from co-operative enzyme kinetics.

A system like eqn (1) is a Turing system of the first kind. If we take parameters like α to be space dependent, a Turing system of the second kind arises (Hunding, 1987). In the present model, we assume that maternal genes set up gradients from the anterior and posterior pole, and thus α becomes:

$$\alpha = \alpha_0[1 + \varepsilon_1(e^{-a\theta} + e^{-a(\pi-\theta)})]. \tag{4}$$

Here, θ is the polar angle from the anterior to the posterior pole of the imposed 3-D prolate spheroidal co-ordinate system (see below). The constant a is chosen such that the anterior gradient follows the experimentally recorded distribution for *bicoid* protein (Driever & Nüsslein-Volhard, 1988). When parameters α_0 and diffusion constants D_1 and D_2 are chosen so that a biperoid pattern of the form $\cos(4\theta)$ may arise in the embryo, the Turing system of the first kind yields a patchy pattern, whereas the introduction of a space dependent rate constant stabilizes a banded pattern, as described in the text and in (Fig. 1). Parameters used for (Fig. 1) are $D_1 = 0{\cdot}08$, $D_2 = 0{\cdot}1 * D_1$, $\alpha_0 = 0{\cdot}35$.

In the next hierarchy of RD systems we use the same idea. A similar RD system is used, with β substituted for α, and β given spatially by the banded gap gene prepattern and maternal gradients:

$$\beta = \beta_0[1 + \varepsilon_1(e^{-a\theta} + e^{-a(\pi-\theta)} + \varepsilon_2 \cos(4\theta))]. \tag{5}$$

When rate constant β_0 and diffusion constants are chosen so that short wavelength patterns may arise in such a system, a highly patchy pattern is obtained, if the epsilons are zero (i.e. no maternal or gap gene control imposed). If ε_1 is non-zero but ε_2 is zero, i.e. maternal double gradients are present, but no double period influence from the gap gene prepattern to the system, then a patchy short wave length prepattern still arises. Thus, the influence from $\cos(4\theta)$ is needed to stabilize the short wave length primary pair-rule prepattern: maternal control is not enough, but gap gene control is needed as well.

When the seven stripes have formed, the maternal gradients may gradually be taken out again of the expression for rate constant β, and thus two new stripes begin to form adjacent to the original seven, compare text and (Fig. 2). Parameters used in (Fig. 2) are $D_1 = 0{\cdot}0012$, $D_2 = 0{\cdot}00012$, $\beta_0 = 0{\cdot}27$, $\varepsilon_1 = 0{\cdot}8$ decreasing to $0{\cdot}1$, and $\varepsilon_1 * \varepsilon_2 = 0{\cdot}4$.

To make stripes, which bend in the dorsal-ventral co-ordinate, diffusion constants may be taken to depend on the DV position, compare (Fig. 4). We imposed a cosine function with amplitude $0{\cdot}35$ on D to vary effective diffusion from $0{\cdot}65$ to $1{\cdot}35$ times the previous value (Fig. 2) of $0{\cdot}0012$.

The Laplacian in three-dimensional prolate spheroidal co-ordinates is

$$\Delta = \frac{4/d^2}{\xi^2 - \cos^2\theta}\left[\frac{\partial}{\partial\xi}(\xi^2-1)\frac{\partial}{\partial\xi} + \frac{1}{\sin\theta}\frac{\partial}{\partial\theta}\sin\theta\frac{\partial}{\partial\theta} + \frac{\xi^2-\cos^2\theta}{(\xi^2-1)\sin^2\theta}\frac{\partial^2}{\partial\phi^2}\right], \quad (6)$$

where d is the interfocal distance, $\xi = (r_1 + r_2)/d$ and $\theta = \cos^{-1}\eta$ with $\eta = (r_1 - r_2)/d$. The corresponding Laplacian for elliptical cylinder co-ordinates is analogous, as it contains the terms for two-dimensional elliptical co-ordinates, and the third term is simply replaced by the double derivative in the cylinder co-ordinate $\partial^2/\partial z^2$. All simulations were made with the longest axis of the embryo set to one.

The numerical solution was achieved as earlier described (Hunding, 1983). Thus the 3-D Laplacian was discretized, and the resulting large number of ordinary non-linear differential equations were solved by a stiff ODE solver, in combination with fast build in sparse matrix iteration codes to handle the corrector step. Red-black (RB, or chessboard) ordering was used to yield a fully vectorizable code, especially suited for modern high speed vector supercomputers. Thus the local integration error is checked in each of the thousands of mesh points in each integration step in order to avoid instabilities and emergence of possible computer artefacts, which demonstrably arise in codes without such a check. A huge speed up over non-stiff algorithms is achieved: The stiff code runs 500 times faster than the non-stiff code, and with the RB vector code an impressive speed up of 12 500 was achieved. As the Amdahl VP 1100 supercomputer used is 15-25 faster already in scalar mode than most department computers, a total speed up of 250 000 over such machines is achieved. Roughly speaking, this changes half a years computer time into one second. This makes realistic 3-D simulations of *Drosophila* prepatterns possible.

For the mathematically oriented reader, we give an outline of the arguments which demonstrate that Turing structures are heavily dependent on boundary conditions, and the fact that a particular pattern or pattern transition usually is common to a large number of different chemical mechanisms.

Reaction-diffusion systems of the form in eqn (1), have a homogeneous stationary state $\mathbf{c}_0$, that is $\partial\mathbf{c}/\partial t = \mathbf{F}(\mathbf{c}_0) = 0$. If $\mathbf{c}$ is expanded in a small parameter ε from $\mathbf{c}_0$, that is $\mathbf{z} = \mathbf{c} - \mathbf{c}_0$, and $\mathbf{z} = \sum \varepsilon^i \phi_i$, we may write eqn (1) in the stationary case in the form of a linear and a remaining non-linear term

$$0 = Lz + N(z) \quad (7)$$

where

$$Lz = Mz + D\Delta z, \quad (8)$$

and M is the Jacobian matrix $\partial\mathbf{F}/\partial\mathbf{c}$ evaluated at $\mathbf{c} = \mathbf{c}_0$. M depends on the rate constants of the mechanism. Turing structures may emerge through bifurcation, if the linear problem $Lz = 0$ also admits non-trivial solutions $z \neq 0$ ($z = 0$ being the homogeneous state), which satisfy the boundary conditions $\partial z/\partial r = 0$, i.e. there is no diffusion transport of the Turing substances over the surface of the embryo. This may happen for particular choices of the rate constants.

For example, for Sel'kovs mechanism, L has the form

$$L=\begin{pmatrix}-1 & -\gamma \\ \alpha & \alpha(\gamma-1)\end{pmatrix}+D\Delta. \tag{9}$$

Candidates for functions which satisfy the boundary conditions are the eigenfunctions ψ of the Laplacian satisfying

$$\Delta\psi_{nlm}=-\kappa^2_{nlm}\psi_{nlm}, \tag{10}$$

and

$$\partial\psi_{nlm}/\partial r=0. \tag{11}$$

If we put

$$z=\begin{pmatrix}\delta_1 \\ \delta_2\end{pmatrix}\psi_{nlm}, \tag{12}$$

to first order in ε, the problem $Lz=0$ has non-zero solutions provided

$$\begin{pmatrix}-1-\kappa^2_{nlm}D_1 & -\gamma \\ \alpha & \alpha(\gamma-1)-\kappa^2_{nlm}D_2\end{pmatrix}\begin{pmatrix}\delta_1 \\ \delta_2\end{pmatrix}=0, \tag{13}$$

which happens when the determinant of the matrix is zero. Thus, from

$$\det\left[M(\alpha)-D\kappa^2_{nlm}\right]=0, \tag{14}$$

we obtain the critical rate constant α_c, which in this case is evaluated as

$$\alpha_c(nlm)=\frac{D_2}{D_1}\,\frac{D_1^2\kappa^4_{nlm}+D_1\kappa^2_{nlm}}{(\gamma-1)D_1\kappa^2_{nlm}-1}. \tag{15}$$

In the general case, a similar determinant equation defines the critical value of a rate constant of the mechanism chosen. For rate constants larger than this critical value, bifurcation from the homogeneous state may take place to inhomogeneous solutions. Equations (13) and (10) show, that a certain pattern, described by ψ_{nlm} and thus κ_{nlm}, obtains when a particular critical $\alpha_c(nlm)$ is reached. However, another pattern $\psi_{n'l'm'}$ obtains, if its characteristic number $\kappa_{n'l'm'}$ is substituted in eqn (13), and the corresponding rate constant $\alpha_c(n'l'm')$, evaluated from eqn (15) is used instead. Moreover, a particular pattern of the form ψ_{nlm} obtained with one chemical mechanism may obtain as well with another chemical mechanism: if κ_{nlm} is substituted into eqn (14) for this *new* mechanism, it is easy to evaluate the parameters for this mechanism, which will give rise to the *same* pattern ψ_{nlm}. Also, the three-dimensional shape of the pattern is defined by the ψ_{nlm} functions, i.e. the eigenfunctions of the Laplacian, rather than on chemical kinetic details.

The above remarks are based on simple linear stability analysis. Actual non-linear bifurcation theory confirms the above analysis, and the independence (in the sense above) of the generated patterns with respect to chemical kinetic details. This holds even in more complicated cases, such as those involving selection rules which determine the particular pattern that arises, when the chosen rate constants allow

more than one pattern. The interested reader is referred to (Hunding, 1982) for details and further references.

It is perhaps necessary to repeat the statement from the main text, however, that this independence of chemical detail obtains when the amplitude of the generated pattern is given sufficiently accurately by the first order term in the above analysis. This is usually the case even for Turing systems, where the ratio of the low to the high concentrations is as high as a factor 5. For very high ratios, which usually obtain when one concentration approaches zero in certain regions, chemical details may become important. Such systems are hard to handle in computer simulations, however, and often require non-standard *ad hoc* computer code, which increases the possibility of generating computer artefacts. Our code, on the contrary, is based on well tested numerical methods which have proved themselves in other fields like fluid mechanics, and previous results with this code have been compared successfully with analytically obtained results.

We shall conclude with a remark about the actual mechanism behind the emergence of Turing structures. There is no such thing as an area of inhibitor which contains trapped spots of activator. According to eqn (13), both components of the mechanism in question have the *same* wave number (proportional to κ_{nlm}) and are thus described by the same function in space ψ_{nlm}. Thus, even in explicit activator/inhibitor mechanisms, the regions where the activator has high concentration *coincide* with the regions where the inhibitor is large. Actually, Turing systems are far more general than chemical mechanisms with explicit activation and inhibition, and we may add that simple "intuitive understanding" of why certain Turing structures emerge instead of others is usually unfounded. Generally, the behaviour of non-linear systems is often surprisingly counter intuitive. Thus, so far no explanation is offered for the observation that the introduction of gradients in a Turing mechanism favours and stabilizes stripes rather than a patchy pattern.

NOTE: Calculations were made using the AMDAHL VP1100 supercomputer of UNI*C, Copenhagen with support from the Danish National Research Council under grant no. 11-7999.